Modulational instability in a silicon-on-insulator directional coupler: role of the coupling-induced group velocity dispersion

W. Ding,[1,*] O. K. Staines,[1] G. D. Hobbs,[1] A. V. Gorbach,[1] C. de Nobriga,[1] W. J. Wadsworth,[1] J. C. Knight,[1] D. V. Skryabin,[1] M. J. Strain,[2] M. Sorel,[2] and R. M. De La Rue[2,3]

[1]*Centre for Photonics and Photonic Materials, Department of Physics, University of Bath, Bath BA2 7AY, UK*

[2]*Optoelectronics Research Group, School of Engineering, University of Glasgow, Glasgow G12 8LT, UK*

[3]*Photonics Research Centre, Physics Department, University of Malaya, 50603 Kuala Lumpur, Malaysia*

**Corresponding author: wding@iphy.ac.cn*

Received October 19, 2011; revised December 8, 2011; accepted December 14, 2011; posted December 14, 2011 (Doc. ID 156580); published February 14, 2012

We report frequency conversion experiments in silicon-on-insulator (SOI) directional couplers. We demonstrate that the evanescent coupling between two subwavelength SOI waveguides is strongly dispersive and significantly modifies modulational instability (MI) spectra through the coupling induced group velocity dispersion (GVD). As the separation between two 380-nm-wide silicon photonic wires decreases, the increasing dispersion of the coupling makes the GVD in the symmetric supermode more normal and suppresses the bandwidth of the MI gain observed for larger separations. © 2012 Optical Society of America

Four-wave mixing (FWM) has been extensively explored in optical fibers and more recently in on-chip silicon-on-insulator (SOI) waveguides (photonic wires), see, e.g., [1–6]. FWM is a cornerstone phenomenon, which has been used in signal processing [3], generation of correlated photon pairs [4], and for fundamental studies of nonlinear waves and solitons [7]. A particular case of FWM with a pair of degenerate pump photons generating and amplifying signal and idler beams is often referred to as modulational instability (MI), which can be either seeded, with signal or idler beams taken from an external source and triggering the process, or spontaneous. In this Letter, we are dealing with the former situation. Directional waveguide couplers and waveguide arrays have attracted detailed attention for light switching, discrete solitons, numerous analogies with electron dynamics in condensed matter [8], and more recently for quantum effects [9]. Therefore, a combination of spatial dynamics and MI in SOI photonic wire couplers and arrays can lead to new developments in nonlinear and quantum applications.

The theory of FWM in directional couplers is described in detail in [10]. However, its experimental realization has not been previously reported. Following recent successes with observation of FWM and MI in single SOI wires [1–6], we have theoretically and numerically investigated this effect in wire arrays [11]. In particular, we have reported that the relatively weak evanescent coupling between the neighboring waveguides can be strongly dispersive [11], so that the coupling induced group velocity dispersion (GVD) can compete with and exceed in value the GVD of a single waveguide. This effect has been observed in the dispersion measurements of slot waveguides [12] and it creates a new, previously unexplored degree of freedom to control FWM and other dispersion-dependent linear, nonlinear, and quantum processes.

In the following, we report the first observations of MI in directional SOI couplers and show how the MI spectrum can be controlled by changing the waveguide separation. We focus on the coupling-induced changes of GVD in the symmetric supermode, in which both waveguides are excited in phase. Our SOI waveguides [see the inset in Fig. 1(b)], are fabricated using electron beam lithography and inductively coupled plasma reactive ion etching. The silicon layer is 220 nm thick and has a 100 nm layer of HSQ resist on its top. The mode of interest is the quasi-TE one with the dominant electric field component parallel to the substrate. Our dispersion measurements have been carried out in a free-space Mach–Zehnder interferometer. Figure 1(a) shows measurements of the relative group index (speed of light

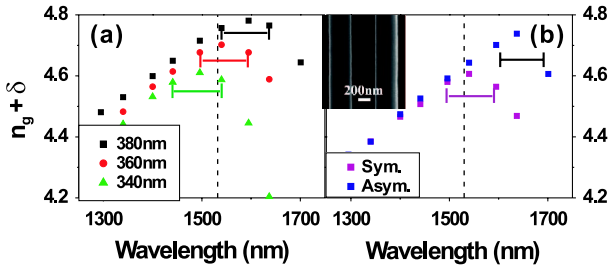

Fig. 1. (Color online) Group indexes, n_g, of the (a) isolated SOI wires and the (b) directional coupler. The widths of the wires in (a) are 340 nm (blue circles), 360 nm (red squares), and 380 nm (black triangles). Two sets of data in (b) correspond to the group indexes of the symmetric and antisymmetric supermodes in a directional coupler (see the inset) of two 380-nm-wide wires separated by a distance of ≃400 nm. The three sets of data in (a) are shifted upward by the different (measurement specific) shifts δ_i with respect to the true values of n_g, while the two lines in (b) are shifted by the same δ. The intervals within which the zero GVD wavelengths are located are indicated with the horizontal bars.

0146-9592/12/040668-03$15.00/0

divided by the group velocity) in isolated SOI waveguides of varying widths. Maxima of these plots correspond to the locations of the zero GVD wavelengths. Dots on the graphs mark all the wavelengths at which measurements have been taken. For example, for the 340-nm-wide waveguides, the zero GVD is located between 1440 and 1540 nm, while for the 380-nm-wide wire, it is between 1540 and 1640 nm. The pump wavelength of 1532 nm is within the range of anomalous GVD for the 360- and 380-nm-wide wires and is within the normal GVD range for the 340 nm one. Numerically simulated dispersion curves for these samples are not able to provide more reliable predictions of the zero GVD location due to uncertainties in the material dispersions and in the geometrical dimensions.

For the directional couplers, we have chosen 380-nm-wide wires separated by 900, 800, and 400 nm distances. An isolated 380-nm-wide wire has a very substantial anomalous GVD at 1530 nm, which is estimated at 2500 ps/nm/km. For the coupler with a separation distance of ≃400 nm, our dispersion measurements allow us to derive maximal and minimal values of group index. Note that the supermodes of the coupler with the 400 nm separation can still be well presented as linear superpositions of the single waveguide modes. According to our previous calculations and experiments [12], we associate the highest group index with the antisymmetric supermode of the coupler and the lowest one with the symmetric supermode. One can see that the zero GVD wavelength of the latter is located between 1500 and 1600 nm, while the former has it above 1540 nm. This pronounced shift of the zero GVD wavelength is attributed to the fact that, for the symmetric supermode, the large normal dispersion of the coupling adds up to the anomalous dispersion of an isolated wire, while, for the antisymmetric supermode, the coupling GVD is subtracted from that of the single wire [11]. The observed changes in GVD are naturally expected to have a strong impact on our MI experiments described below. Our measurements cannot tell with certainty if, at the pump wavelength of 1530 nm, the 400 nm coupler has normal or anomalous GVD. The MI experiments described below favor the anomalous GVD values: 380-nm-wide waveguides separated by 800 and 900 nm have the group indexes (not shown) very close to the single waveguide one, so that the splitting between GVDs of the two supermodes is negligible and hence MI develops similarly to the single wire waveguides.

MI experiments were performed using the setup shown in Fig. 2(a). The pump (at 1532 or 1530 nm) and the signal (on the short wavelength side from the pump) pulses are both derived from a 250 KHz femtosecond pulse train. After a transmission grating, part of the light is passed through a two-stage erbium-doped fiber amplifier and the amplifier noise is then eliminated using a bandpass filter. Care has been taken to minimize the chirp of the pump pulses. The measured autocorrelation trace is shown in the inset of Fig. 2(a) and implies a pulse duration of 8.5 ps. For such a long pulse, the dispersive pulse spreading inside the wires can be ignored. On the other path, the generated and seeded signal pulses are coupled into a 10-m-long hollow-core photonic crystal fiber followed by a movable translation stage. Such an

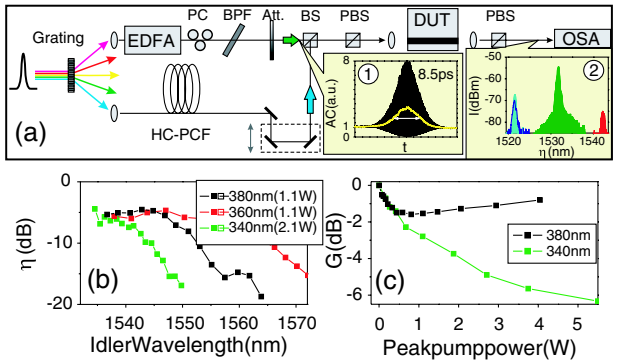

Fig. 2. (Color online) (a) Experimental setup. Inset 1: interferometric autocorrelation trace of the input pump pulses. Inset 2: a typical output spectrum includes pump (green), signal (blue), and idler (red) peaks. The light (dark) blue curve represents the signal output with the pump off (on). PC, polarization controller; BS, beam splitter; PBS, polarized beam splitter; DUT, device (photonic wires) under test. (b) Measured conversion efficiency spectra of three single-channel waveguides (widths: 380, 360, and 340 nm, respectively) with the pump at 1532 nm. The peak pump power inside the waveguide is shown in the label. (c) MI gain versus peak pump power inside the 380-nm-wide (black, $\lambda_{\text{signal}} = 1520$ nm) and 340-nm-wide (blue, $\lambda_{\text{signal}} = 1518$ nm) wires. The peak signal power inside the wires is ≃0.15 W.

arrangement enables us to compensate the large time delay accumulated in the pump route with negligible dispersion and nonlinearity. In the end, the pump and signal pulses are combined, coupled into the SOI wires with TE polarization, and then measured by using an optical spectrum analyzer. The in-coupling section of the setup totally consists of free-space optics, thus avoiding any other nonlinear process except that in the test waveguide. Inset 2 in Fig. 2(a) shows a typical output spectrum. The idler peak (at 1542 nm) appears only when the pump (at 1532 nm) and the signal (at 1522 nm) pulses are simultaneously sent into the waveguide.

We define conversion efficiency η as the converted idler power divided by the signal power in the output, and MI gain G as the signal power with the pump switched on divided by that with the pump off: $\eta = P^{\text{out}}_{\text{idler}}/P^{\text{in}}_{\text{signal}}$, $G = P^{\text{out}}_{\text{signal}}(\text{pump on})/P^{\text{out}}_{\text{signal}}(\text{pump of}f)$. We present data showing η as a function of the idler wavelength and G as a function of the pump power, see Figs. 2,3. In order to make interpretation of our measurements with couplers transparent we need to discuss the single wire experiments first. Figure 2(b) shows the measured conversion efficiency spectra. The in-coupling lens has an NA of 0.65 and we expect a coupling loss of 8.5–11.5 dB depending on the waveguide width and the quality of the sample facet. The peak power of the pump pulse inside the waveguide is estimated and labeled in the plot. At these powers, the self-phase modulation does not cause significant spectral broadening and asymmetry. As the waveguide width varies from ≃340 to ≃380 nm, the GVD at the pump wavelength 1532 nm changes from being normal to anomalous. The conversion bandwidth Δ in the small-gain limit and neglecting higher-order dispersions can be approximated as $\Delta = \sqrt{4\pi/(|\beta_2|L)}$ [5], where β_2 is the GVD coefficient and L

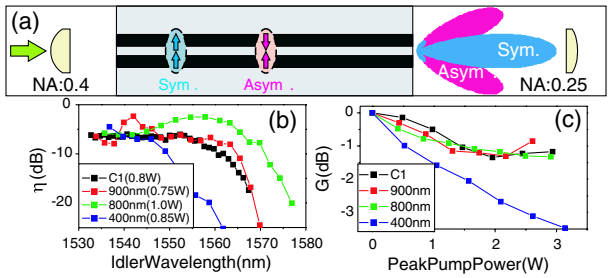

Fig. 3. (Color online) (a) Supermode excitation and collection in a directional SOI coupler. The radiation patterns of the symmetric and asymmetric supermodes are also shown. (b) Conversion efficiency versus idler wavelength in the couplers with separation distances 900, 800, and 400 nm. Estimated peak pump powers inside the waveguides are given in the label. (c) MI gain versus peak pump power of the arrays with $\lambda_{\text{pump}} = 1530$ nm and $\lambda_{\text{signal}} = 1518$ nm.

is the propagation distance. The wire width 360 nm exhibits the broadest MI conversion band and, thus, the expected absolute value of GVD is smallest. In order to determine if the converted spectrum experiences any MI gain, we measured the dependence of the gain parameter G on the pump power for the widest (380 nm) and narrowest (340 nm) wires, see Fig. 2(c). For small pump powers, the dominant process at the signal wavelength in both wires is the cross-phase modulation (XPM)-induced spectral broadening accompanied by two-photon and free carrier absorption [13], which cause the drop in the gain. For larger pump powers the gain behaves differently in the two waveguides. For the 380-nm-wide wire, we observe that the initial drop of G is followed by the rise occurring at the pump power of 0.5 W. This rise is associated with the MI gain starting to counter balance all the loss mechanisms. On the other hand, if the GVD at the pump wavelength is large and normal, as in the 340 nm waveguide, the MI gain is absent, and spectra are dominated by the XPM related broadening and by damping, so that G shows a continuous drop with the increasing pump power.

In the MI experiments with couplers, we have taken care to excite and detect, primarily, the symmetric supermode inside the couplers, using suitable in- and out-coupling lenses and adjusting the input beam maximum between the waveguides, see Fig. 3(a). Thus, we exclude any possible instabilities associated with the nonlinear cross coupling between the supermodes [14]. The length of the coupler is 3.3 mm, and we estimate the coupling lengths at 1530 nm to be 3.5, 1.7, and 0.1 mm for the separations 900, 800, and 400 nm, respectively. The corresponding critical powers associated with the symmetry-breaking bifurcation of the symmetric supermode [10] are 500, 30, and 15 W, respectively. Figure 3(b) shows the conversion efficiency spectra observed for the pump wavelength at 1530 nm and Fig. 3(c) shows the MI gain versus pump power. For large separations of 800 and 900 nm, both dependencies are very similar to the ones observed in single waveguides and correspond to the presence of the MI-generating parametric gain. GVD in the symmetric supermode in these cases is anomalous at 1530 nm. For the waveguide separation 400 nm, we have observed the narrowing of conversion efficiency spectra and gain measurements continuously decreasing with pump power, see Figs. 3(b,c), which unambiguously indicates that the MI process is not present. This is a strong argument that the pump wavelength GVD in this coupler, which could not be determined with certainty through our linear measurements (see discussion above), is actually normal. Note that the length of the chip with couplers (3.3 mm) is significantly shorter than that with the isolated wires (5.5 mm), which explains why the minimum of the gain curve in Fig. 3(c) occurs at greater pump powers compared to Fig. 2(c).

In summary, we have investigated the MI process in directional couplers of SOI photonic wires and demonstrated its pronounced dependence on the coupling induced GVD. Our observations open opportunities for development of new methods of controlling dispersion and frequency conversion in subwavelength waveguides.

Support from the Engineering and Physical Sciences Research Council project EP/G044163/1 is acknowledged.

References

1. H. Fukuda, K. Yamada, T. Shoji, M. Takahashi, T. Tsuchizawa, T. Watanabe, J. Takahashi, and S. Itabashi, Opt. Express **13**, 4629 (2005).
2. M. A. Foster, A. C. Turner, J. E. Sharping, B. S. Schmidt, M. Lipson, and A. L. Gaeta, Nature **441**, 960 (2006).
3. C. Koos, P. Vorreau, T. Vallaitis, P. Dumon, W. Bogaerts, R. Baets, B. Esembeson, I. Biaggio, T. Michinobu, F. Diederich, W. Freude, and J. Leuthold, Nat. Photon. **3**, 216 (2009).
4. J. E. Sharping, K. F. Lee, M. A. Foster, A. C. Turner, B. S. Schmidt, M. Lipson, A. L. Gaeta, and P. Kumar, Opt. Express **14**, 12388 (2006).
5. M. A. Foster, A. C. Turner, R. Salem, M. Lipson, and A. L. Gaeta, Opt. Express **15**, 12949 (2007).
6. A. C. Turner-Foster, M. A. Foster, R. Salem, A. L. Gaeta, and M. Lipson, Opt. Express **18**, 1904 (2010).
7. B. Kibler, J. Fatome, C. Finot, G. Millot, F. Dias, G. Genty, N. Akhmediev, and J. M. Dudley, Nat. Phys. **6**, 790 (2010).
8. F. Lederer, G. I. Stegeman, D. N. Christodoulides, G. Assanto, M. Segev, and Y. Silberberg, Phys. Rep. **463**, 1 (2008).
9. Y. Bromberg, Y. Lahini, and Y. Silberberg, Phys. Rev. Lett. **105**, 263604 (2010).
10. G. P. Agrawal, *Applications of Nonlinear Optics* (Academic, 2001).
11. C. J. Benton and D. V. Skryabin, Opt. Express **17**, 5879 (2009).
12. C. E. de Nobriga, G. D. Hobbs, W. J. Wadsworth, J. C. Knight, D. V. Skryabin, A. Samarelli, M. Sorel, and R. M. De La Rue, Opt. Lett. **35**, 3925 (2010).
13. I. W. Hsieh, X. G. Chen, J. I. Dadap, N. C. Panoiu, and R. M. Osgood, Jr., Opt. Express **15**, 1135 (2007).
14. S. Trillo, S. Wabnitz, G. I. Stegeman, and E. M. Wright, J. Opt. Soc. Am. B **6**, 889 (1989).